PARAMETROS DE FRACTURA PARA MATERIALES PETREOS: COMPARACION DE LOS RESULTADOS OBTENIDOS APLICANDO DISTINTOS PROCEDIMIENTOS

FRACTURE PARAMETERS OF ROCK MATERIALS: A COMPARISON OF RESULTS FROM AVAILABLE MODELS.

A. Fathy, J. Planas and M. Elices
Departamento de Ciencia de Materiales. E.T.S. Ingenieros de Caminos.
Universidad Politécnica de Madrid. Ciudad Universitaria. 28040-MADRID.

Resumen.- Se han propuestos diversos parámetros para caracterizar la fractura de los materiales pétreos, ya que la mecánica de la fractura en régimen elástico y lineal no parece que sea aplicable en las condiciones usuales de laboratorios. En esta comunicación se han ensayado probetas entalladas de mármol y de granito y se han registrado la curva carga-desplazamiento y carga-CMOD hasta la iniciación de la rotura y durante la propagación estable de la fisura.
A partir de estos datos se han determinado los parámetros de fractura aplicando distintos procedimientos: (a) El método de Bazant. (b) El método de Shah (de los dos parámetros). (c) El método de Karihaloo. (d) El método RILEM.
Los resultados que se obtienen son distintos y en la comunicación se analizan las posibles causas de estas diferencias.

Abstract.- The purpose of this study is to provide comparisons between various existing methods for the evaluation of fracture parameters taking non-linear effects into account for quasi-brittle materials.
Experimental results of notched three point bend tests of granite and marble materials were interpreted according to three non-linear fracture models in order to get fracture mechanical parameters, independent on specimen size. The possible mechanism of size effect for rocks with a discussion of the usefulness of these methods are presented.

1. INTRODUCTION

In the last decade, many attempts have been made to define fracture parameters for quasi brittle materials, such as concrete, rocks and ceramics, in substitution of the usual linear elastic fracture mechanics (LEFM) parameters, because it turned out that laboratory specimens were too small for LEFM to apply [1].

Besides the RILEM proposed method [2, 3], three other models have been checked to determine size independent fracture parameters: Bazant's [4, 5], Jenq and Shah's [6, 7], and Nallathambi and Karihaloo's [8, 9]. All these models intend to account for the non-linear behaviour of quasi brittle materials around the crack tip region .

In order to investigate the validity of these proposals for rocks, a series of experiments on granite and marble were conducted on notched beams. Since most recent researches showed that there is a dependence of results upon specimen dimensions, beams of various sizes and thicknesses were tested. In section 2, the experimental procedures are described, followed in section 3, by a brief account of the applied models, with emphasis on the fulfilment of experimental requirements for their applicability. In section 4, the results are presented and discussed, and the main conclusions are summarized in section 5.

2. EXPERIMENTAL PROCEDURES.

2.1. Test specimens

Fracture specimens were three point bend notched beams as shown in fig. 1. All specimens had a notch to depth ratio of 0.5 and a span to depth ratio of 4.

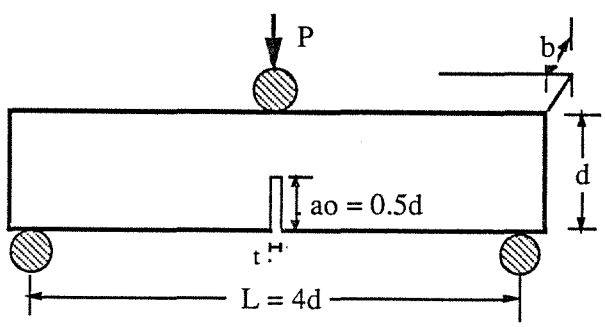

Fig. 1. TPB specimen geometry.

In order to minimize the possible influence of anisotropy, and nonhomogenuity, all the specimens were cut from a single block of rock, and the orientation of the crack plane was carefully kept fixed in all specimens.

Specimens of four different sizes in proportions 1: 2: 4: 8 were used to investigate the size effect. The actual sizes are listed in table 1. They were chosen to have minimum specimen dimension exceeding 5 times the maximum grain size. The notches were sawn using a diamond disk and a diamond wire, resulting in notch widths of 1.2 and 0.15 mm, respectively. The smallest specimens were always wire-sawn, while the larger ones were mainly disk-sawn because a preliminary test series showed that the results were unaffected by the notch width in this range.

In order to investigate the effect of the specimen thickness on the results, three beam thicknesses were tested (b= 30, 10 and 6 mm).

Table 1. Specimens dimensions.

GROUP	Nominal depth (mm)	Rate of loading (micron/sec.)	CMOD gage length (mm)
I	100	3.00	25
II	50	1.78	12.5
III	25	1.06	6.25
IV	12.5	0.626	3.125

1. b≈ 30, 10 and 6 mm.
2. L = 4 d
3. ao/d = 0.5
4. every group consists of 6 specimens.

Cylindrical test specimens for splitting tensile testing (Brazilian test) were cored from the rock block. At testing, the core specimens were carefully placed to get splitting along planes in the same orientation as the cracking ones of the notched beams.

2.2. Testing machine and test procedure

A servohydraulic testing machine (INSTRON 8501) with CMOD feed back signal was used to perform stable tests fig. 2. The crack mouth opening displacement (CMOD) was recorded using a clip gauge attached directly to the specimen lower face with sharp knife edges and springs. The knife edge separation (CMOD gage length) was roughly proportional to the beam depth (see Table 1). The applied quasi-static load was recorded continuously during the test using a load cell of 10 kN capacity (static). Load was measured with an accuracy of 0.5% of indicated load. The mid-span deflection was measured as the average of the readings of two symmetrically placed displacement transducers. Deflection, CMOD and load were red and stored by a data acquisition system (DAS) until the beam was completely separated into two halves.

The rate of loading for each testing size was chosen to reach the peak load in about 50 to 100 sec. Supports and loading arrangements were such that the acting forces on the beam were statically determinate. The central load was applied through the upper hinge at mid-span, while the two lower rollers were let free after test set up in order to minimize the friction forces. Also, these two lower rollers rested upon cylindrical supports to avoid torsional effects.

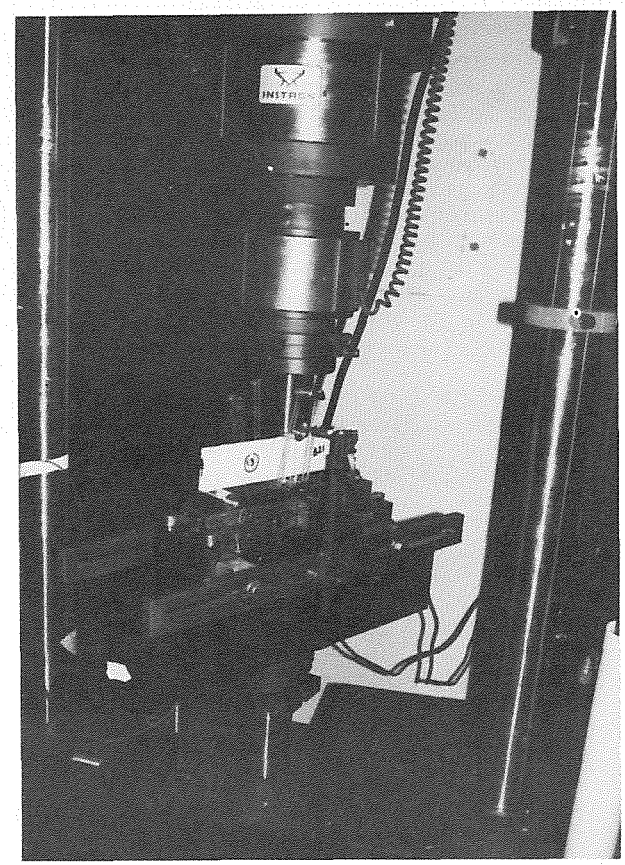

Fig. 2. Test machine and loading arrangement.

The compensation of beam own weight was made by two elastic springs at mid span, a procedure that allows the determination of all the dissipated energy without recourse to theoretical corrections of the results [10].

The effectiveness of such a method was checked by testing another special group having a total length twice the loading span, without hanging neither springs nor CMOD transducer. The typical results assert that there is no weight influence on fracture parameter evaluation for the experimental technique used in our tests.

3. APPLIED MODELS.

3.1. Fictitious crack model by Hillerborg

The fictitious crack model was proposed by Hillerborg for predicting crack growth behaviour of concrete in 1976. The fracture process zone is modelled as an extension of the actual crack subjected to closing forces which depend on the crack opening displacement in a unique way. Consequently, the tensile strength and the fracture energy G_F are material properties [1]. An indirect method for measuring the fracture energy G_F was developed by Hillerborg *et al.* [2, 3, 11], using three point bend notched beam specimens. The area under the load-deformation curve is measured to represent the energy dissipated in fracturing the specimen. The fracture energy G_F follows by dividing the total energy by the initial ligament area.

3.2. Size effect law by Bazant

The fracture energy G_F obtained by this method is defined as the specific energy required for fracture growth in an infinitely large test specimen. Description and details of test method can be found in the draft recommendation [5]. These recommendations were followed throughout the testing, except for a few particular aspects. If one identifies the maximum aggregate size of concrete (the RILEM recommendation is only for concrete) as the maximum grain size for rock, then some notches were wider than those recommended (1/2 of grain size). But, as already stated in 2.1. preliminary tests showed that the results unaffected by using a notch width of 1.2 mm.

The smaller depth size was recommended not to exceed 5 times the maximum aggregate size. However, this leads to exceedingly small specimens for our rocks, the minimum practical size for our testing set up being of the order of 10 mm.

The last deviation regards the testing rate, which was about 5 times faster than in this recommendation. This was so because the rate was chosen to comply with the fracture energy RILEM recommendation [2].

3.3. Two parameter fracture model by Jenq and Shah

The two parameter model is at the base of a method, which allows the determination of the material toughness K^s_{Ic} and the critical crack tip opening displacement $CTOD_c$. See recommendation draft [7] for details.

All the essential requirements stated by this proposal were achieved, but :
1) Notch to depth ratio a_0/d was 1/2 instead of 1/3.
2) The peak load was reached about ≈100 sec. after test initiation, while 5 minutes are suggested in the recommendation.
3) No unloading-reloading was made to evaluate stable crack growth. However, as indicated in the same recommendation, linear unloading path from the peak load point to the origin may be assumed when no unloading is possible or wanted, with may be an accuracy loss of about 20%.

3.4. Effective crack model by Nallathambi and Karihaloo

Apart from the procedure used to determine the effective crack length, this procedure is similar to the former of Jenq and Shah. The load-deflection curve is used instead of the load-CMOD curve to find the effective crack extension. Specimen and test requirements are the same as before.

See ref. [9] for details in the determination of the fracture toughness K^e_{Ic} given by this method.

4. TEST RESULTS AND DISCUSSION.

4.1. Tensile strength and Young's modulus.

Average values of tensile strength (f_t), obtained from Brazilian tests on 50 mm diameter cores, and the modulus of elasticity (E) calculated from the initial slope of the load-CMOD curves using Tada's formula [12], are shown in table 2. Values of the standard deviation are shown in parentheses.

Table 2. Young's modulus and tensile strength.

Material	E (GPa)	f_t (MPa)
Marble	36 (7)	7.7 (0.8)
Granite	39 (4)	12.3 (1.3)

4.2. Influence of specimen thickness

Since the peak load is the essential experimental result for the obtention of fracture parameters following Bazant's, Shah's and Karihaloo's methods, the thickness effect on fracture parameters evaluated by these methods was investigated by comparing the strengths for different thicknesses: for a given size (beam depth), we define a relative strength μ as the ratio of the peak load per unit thickness for every specimen by the average peak load per unit thickness for the thicker specimens (30 mm thickness), i.e.,

$$\mu = \frac{b_{max}\, P_{peack}(b)}{b \left\langle P_{peak}(b_{max}) \right\rangle} \qquad (1)$$

where angle brackets indicate average value. Figs. 3a and 3b show that there is not any significant influence of the thickness on the strength of granite specimens. Marble specimens show a larger scatter and somewhat anomalous results are found for the 6 mm thickness specimens. In a first interpretation, it is possible that some damage was introduced in machining these specimens. Further testing will be made to verify or discard these results.

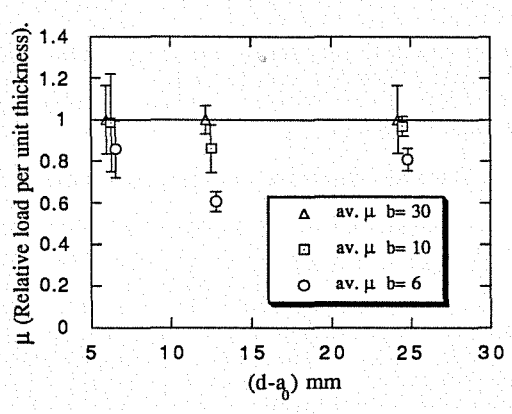

Fig. 3.a Thickness effect upon relative load for marble.

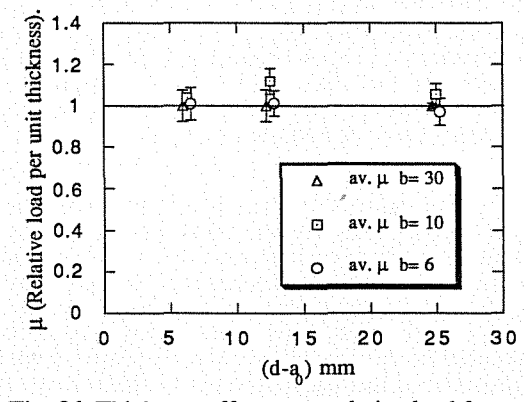

Fig. 3.b Thickness effect upon relative load for granite.

The same procedure may be followed for the fracture energy G_F obtained using Hillerborg method, by defining the relative fracture energy value Ω as

$$\Omega = \frac{G_F(b)}{\langle G_F(b_{max}) \rangle} \qquad (2)$$

Figs 3c an 3d show that the influence of specimen thickness on G_F is not significant, since the differences are attributed to statistical scatter.

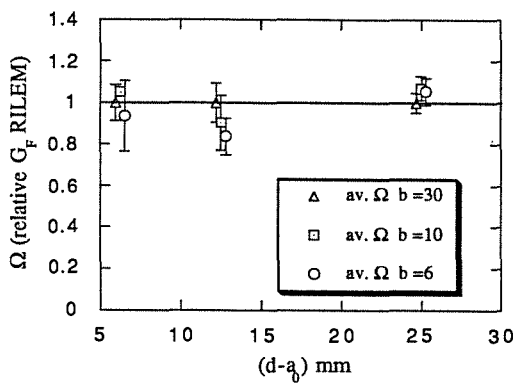

Fig. 3.c Thickness effect upon fracture energy for marble.

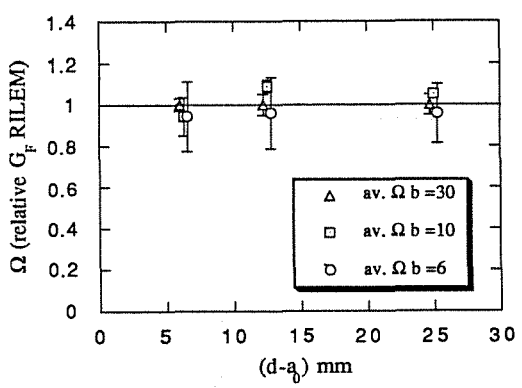

Fig. 3.d Thickness effect upon fracture energy for granite.

4.3. Fracture parameters.

The results of all the methods have been put into a comparable form by transforming the critical stress intensity factors into crack growth resistance or fracture energy, by writing:

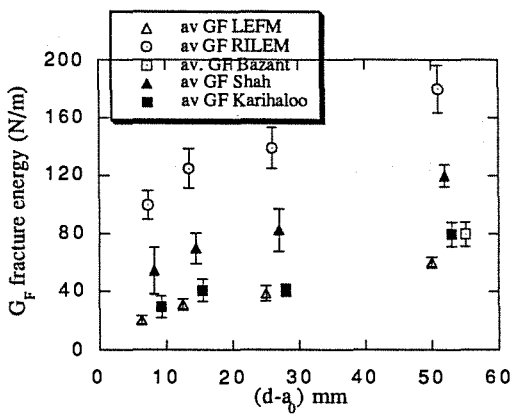

Fig. 4.a Comparison of G_F for marble

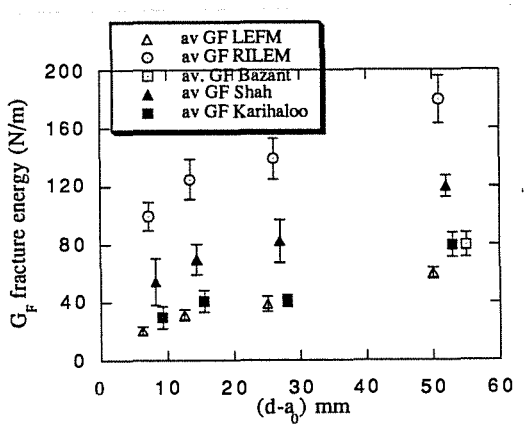

Fig. 4.b Comparison of G_F for granite

Table 3. Comparison of fracture energy.

Material	d nominal depth (mm)	G_F (N/m) RILEM	BAZANT	SHAH	KARIHALOO	LEFM	spec.
Marble	100.0	**141.9**± 7.3	**71.5**± 9.6	**101.1**± 18.8	**46.2**± 7.4	**42.1** ± 5.9	**6**
	50.0	**105.6**± 6.3		**66.0**± 22.8	**29.6**± 4.2	**22.7** ± 5.8	**18**
	25.0	**88.2**± 10.7		**43.7**± 5.9	**28.1**± 7.7	**15.4** ± 4.7	**16**
	12.5	**67.9**± 9.0		**31.4**±7.1	**20.3**± 8.4	**10.4** ± 3.2	**16**
Granite	100.0	**179.6**± 16.2	**79.5**± 8.3	**119.9**± 7.6	**69.5**± 8.3	**60.0** ± 3.9	**6**
	50.0	**139.0**± 14.0		**82.2**± 14.7	**41.0**± 4.2	**38.9** ± 5.4	**14**
	25.0	**124.8**± 13.7		**69.7**± 10.5	**40.9**± 7.8	**31.2** ± 3.8	**15**
	12.5	**99.4**± 9.8		**54.4**± 15.9	**29.6**± 7.6	**20.4** ± 2.9	**13**

$$G_F = \frac{(K_{Ic})^2}{E}$$

In this way, G_F for each model (and experimental method) may be interpreted as the critical energy release rate predicted by each model for specimens of infinite size.

The results of statistical analysis for Bazant's method are shown in table 4. They show that scatter is too high for marble to meet the requirements of the RILEM recommendation, specially for the width of the scatter band (m). This shown in figs. 5a and 5b, where all experimental results are plotted to emphasize the abnormally large scatter for marble. Scatter of granite is high, but reasonable.

Table 4. Statistic coefficients for Bazant method.

Coeifficient	Granite	Marble	Accepted values
(ω_A) coefficient of variation of the slope of the regression line	0.08	0.27	≤ 0.10
(ω_C) coefficient of variation of the intercept	0.09	0.12	≤ 0.20
(m) relative width of scatter band	0.25	0.52	≤ 0.20

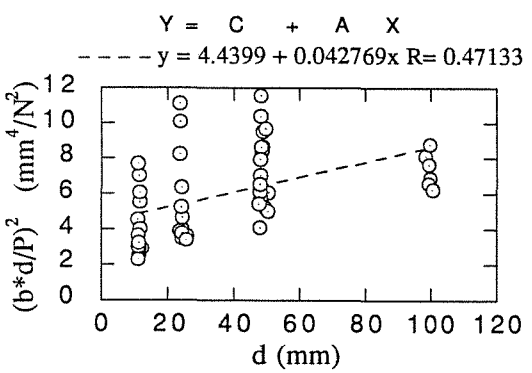

Fig. 5.a Linear regression plot for marble acc. to Bazant.

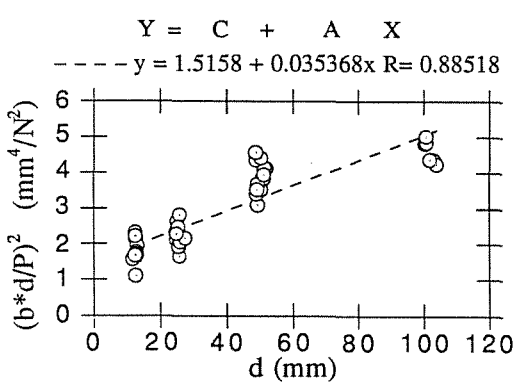

Fig. 5.b Linear regression plot for granite acc. to Bazant.

4.4. Influence of ligament length

From figs. 4a and 4b, the influence of ligament length upon fracture energy measurement is apparent for all the methods (except Bazant's that no rules out any size effect). This size effect may be represented in a different form to put into evidence the amount of size effect in relative terms. For a given size (beam depth) we define a relative energy ß as the ratio of G_F for every specimen by the average G_F of 100 mm depth, i.e.,

$$\beta = \frac{G_F(d)}{\langle G_F(d_{max}) \rangle} \qquad (3)$$

where angle brackets indicate average value. Figs 6a and 6b show plots of the relative fracture energy versus dimensionless ligament size, where the characteristic size l_{ch} was defined as:

$$l_{ch} = \frac{E\langle G_F \rangle}{f_t} \qquad (4)$$

for our purposes, $\langle G_F \rangle$ is the average of the Hillerborg fracture energy for the four sizes.

It may be observed that the size effect is very pronounced, a 2.5 times increase in GF for an 8 fold increase in size. Surprisingly enough, the relative size effect is the same—within scatter— for all models and experimental procedures.

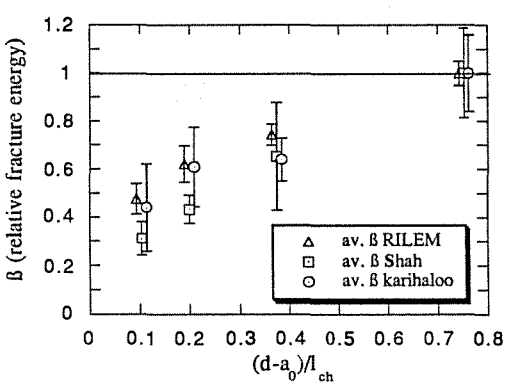

Fig. 6.a Ligament length influence on fracture energy for marble.

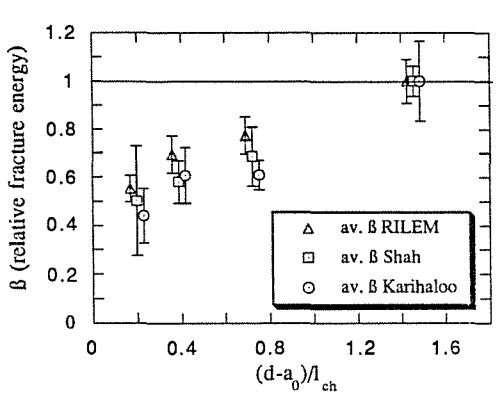

Fig. 6.b Ligament length influence on fracture energy for granite.

5. CONCLUSIONS

1- Fracture parameters, expressed as fracture energy, for five different fracture theories have been determined from the same experimental set for marble and granite.

2- The measured fracture energy for a given material and specimen size is highly dependent on the underlying theory. LEFM gives the lower estimate and the Hillerborg model the highest, in a ratio of 1:3 approximately. Karihaloo's method is very close to LEFM and Shah's and Bazant give values in between.

3- All the methods, except Bazant's, lead to values of the fracture energy that display a strong size dependence. Surprisingly enough, the relative influence of the size is roughly the same whatever the method.

4- The size dependence of the fracture parameters associated to LEFM and to effective crack models like Shah's and Karihaloo's are not very surprising because of well documented existence of large process zone region ahead of the crack, that can be treated in the elastic crack framework only for very large specimens.

5- The size dependence of Hillerborg's G_F, is much harder to explain. The most obvious, but useless approach is to postulate that the cohesive or fictitious crack model is not valid and to look for a better model, with no obvious candidate at hand. A more involved approach is to analyze the experimental technique in depth to try discarding the source of a systematic error in the evaluation of the dissipated energy. Recent results along this line are very promising [14], and push towards pursuing in this later interpretation.

Acknowledgment: The authors gratefully acknowledge financial support for this research provided by CYCYT, Spain, Undergrants PB86-0494 and CE89-0012, and the "Spanish Institute for Cooperation with the Arab World".

6. REFERENCES

1. Elices M. and Planas J.,"Material Models", Chap. 3 in State of the Art Report on Fracture of Concrete, RILEM TC-90, L.Elfgren, Ed., 1988.

2. "Determination of the Fracture Energy of Mortar and Concrete by Means of Three Point Bend Tests on Notched Beams", RILEM Draft Recommendation, Materials and Structures, Vol. 18, No.106, 1985, pp. 285-296.

3. Hillerborg A.E., Modeer M. and Petersson P.E., "Analysis of Crack Formation and Crack Growth in Concrete by Means of Fracture Mechanics and Finite elements", Cement and Concrete Research, Vol.6, 1976, pp. 773-782.

4. Bazant Z.P., and Oh B.H.,"Crack Band Theory for Fracture of Concrete", RILEM, Materials and Structures, Vol. 16, No. 93, May 1983, pp. 155-177.

5. "Size-Effect Method for Determining Fracture Energy and Process Zone Size of Concrete", RILEM Draft Recommendation, TC89-FMT fracture mechanics of concrete test methods, Materials and Structures, 23, pp. 461-465.

6. Jenq Y.S.and Shah S.P.,"Two Parameter Fracture Model for Concrete", Journal of Engineering Mechanics, Div., ASCE, Vol. 111, No. 10, Oct. 1985, pp. 1227-1241.

7. "Determination of Fracture Parameters (KIc and CTODc) of Plain Concrete Using Three-Point Bend Tests", RILEM Draft Recommendation, TC89-FMT fracture mechanics of concrete test methods, Materials and Structures, 23, pp. 457-460.

8. Nallathambi P. and Karihaloo B.L.,"Determination of Specimen Size Independent Fracture Toughness of Plain Concrete", Magazine of Concrete Research, Vol. 38, No. 135, June 1986, pp. 67-76.

9. B.L.Karihaloo, P.Nallathambi, "Fracture of Concrete and Rock", Report presented to RILEM committee 89-FMT, Fracture Mechanics of Concrete: Subcommittee A: Notched beam tests: Mode I Fracture Toughness, 1989.

10. Planas J., and Elices M.,"Conceptual and Experimental Problems in the Determination of the Fracture Energy of Concrete", International workshop on fracture toughness and fracture energy of concrete and rock, Tohoku University, Sendai, Japan, October 12-14, 1988.

11. Hillerborg A.E.,"The Theoretical Basis of a method to Determine the Fracture Energy G_F of Concrete", Materials and Structures, Vol.18, No.107, 1985, pp. 291-296.

12. H. Tada, P. Paris and G. Irwin, "The Stress Analysis Of Cracks Handbook", second edition, Paris Production Incorporated, 1985, pp. -2.16-2.18.

13. J. Planas, and M. Elices, "Toward A Measure of G_F : An Analysis Of Experimental Results", Fracture Toughness and Fracture Energy Of Concrete, edited by F.H.Wittmann, Elsevier Science Publishers B.V., Amsterdam , 1986, pp. 381-395.

14. G.V.Guinea, "Medida de la Energía de Fractura del Hormigon", Tesis Doctoral, Departamento de Ciencía de Materiales, Univ. Politecnica de Madrid, 1990.